

# 17 A parameterization for the turbulent fluxes over melting surfaces derived from eddy correlation measurements

MARKUS WEBER

Commission for Glaciology of the Bavarian Academy of Sciences and Humanities, Alfons-Goppel-Str. 11, D-80539 Munich, Germany

## Abstract

The temperature of a melting surface of snow or ice should never exceed 0°C even if the layer of air above is much warmer. Hence the thermal layering mostly is characterized by a stable state. Under such conditions the exchange of heat and moisture are severely limited because of depauperate turbulence.

During a clear day between 80 and 90 percent of the energy available for melt is delivered by the radiation budget. Almost the complete residual of the surface energy balance is distributed on the turbulent fluxes of sensible and latent heat. Over a period of time with overcast and windy weather the relevance of the turbulent fluxes may rise from 10 to 30 percent and more. Thus the accurate calculation of the turbulent heat fluxes is very important for the melt modelling of water production.

To parameterize turbulent transport processes within the stable stratified surface layer using the *Monin-Obukhov*-similarity theory is inaccurate in contrast to unstable conditions. Catabatic flows generated at inclined areas may raise the efficiency of mixing by forcing mechanical turbulence. Under such conditions, e.g. the presumed invariance of the fluxes with height is definitely violated and therefore the common known scheme is inapplicable.

The analysis of data from *Eddy-Correlation*-measurements over an inclined surface gives an insight to the structure of turbulence within the surface layer. The experiments were carried out in August 1998 (HyMEX98) and August 2000 (HyMEX 2000) at Vernagtferner (Oetztal Alps, Austria). The results presented in this paper show that the integral to the cospectra and thus the cinematic fluxes can be well calculated using the so called "flux-variance relationship". Therefore an approach like a bulk formula can be proved the best fit for parameterization. The amazing analogy of the turbulent structure of the enthalpy distribution, in contrast to that of moisture, suggests that the latent heat flux can be calculated using a similar algorithm.

This contribution shows a workable bulk parameterization scheme to calculate the turbulent fluxes in case of a stable stratified surface layer.

## 1. Introduction

A layer of accumulated snow or ice can basically be ablated by mechanical erosion and by transformation from the solid to the liquid or gaseous state. The latter processes of melting or sublimation require a lot of thermal energy: to melt 1 kg of ice at 0°C an amount of 0.334 MJ of energy is required. To evaporate it, an additional 2.5 MJ is needed. Potential sources of energy are the absorption of long wave and short wave radiation and the turbulent fluxes from the atmosphere. Over snow, the energy sinks are the reflection of the short wave radiation and the emission of long wave radiation at the surface. Advection of very cold or very dry air may result in important losses of energy by turbulent fluxes directed into the atmospheric surface layer. The available energy flux **SE** for phase transformation is determined by the well known surface energy balance equation

$$SE = RB + H + LE + G \quad [Wm^{-2}] \quad [1.1]$$

where **RB** is the radiation balance, **H** the turbulent flux of sensible heat, **LE** that of the latent heat and **G** the heat conduction into or out of the snow pack. During melt conditions it is justified to consider **G** as negligibly small. The term **RB** balances the incoming and outgoing radiative fluxes in the short wave (**S**) and long wave (**L**) range using the commonly known equation

[1.2]

$$RB = (S\downarrow - S\uparrow) + (L\downarrow - L\uparrow) [T_s] \quad [Wm^{-2}]$$

A flux directed from the atmosphere towards the surface is considered positive. Snow- or icemelt, the transition from the solid to the liquid state, occurs only under the condition that the surface temperature rises up to 0°C and the residual **SE** is positive. These conditions are usually associated with positive values of the air temperature above the surface and with a positive radiation balance. In that case each term of the right side of eq. [1.1] is a potential source for melt. In contrast, if the air temperature drops below zero, sublimation represented by the latent heat flux **LE** is the exclusive process, which leads to a mass loss of the snow pack (apart from mechanical erosion, which is not considered here).

Since the consumption of energy to sublimate 1 kg of solid water is more than eight times higher than melt, the latter is the most efficient process to ablate the snow cover in any case. The temperature of a melting surface of snow or ice will never exceed 0°C even if the layer of air above is much warmer. This boundary conditions lead to some interesting implications:

- Unlike other surface types, the very important upper boundary value of the surface temperature is a well known constant without any variation in time.
- The long wave emitted radiation flux  $L\uparrow$  is an important sink for the energy balance and directly dependent on the surface temperature. It never exceeds an upper threshold of approx.  $315 Wm^{-2}$ . The incoming long-wave radiation, however, is dependent on air temperature and humidity (KUZMIN 1961). Advection of

warmer and more humid air will always increase the energy available for melt.

- Thermal layering near the surface is mostly characterized by extreme stable stratification, i.e. air temperature increases with height above ground. Very strong vertical temperature gradients can be found in the magnitude of some K/m. Under such conditions exchange of heat and moisture should be severely limited because of suppressed thermal turbulence. But if turbulent motion is generated mechanically by windshear, friction and so on, the resulting flux of sensible heat is always directed to the surface and therefore an enhancement to the surface energy budget.
- The kind of the contribution – increasing or reducing – of the latent heat flux to the energy balance depends on the humidity conditions. A partial pressure of water vapour below 6.15 hp is leading to losses by evaporation, while a higher content provides additional energy from condensation.
- A deep snow cover smoothes the bumpiness of the underlying surface of an area and therefore decreases its aerodynamic roughness.

The individual contribution of each energy balance component varies in a wide range, which depends on the local conditions. For example the partitioning of energy which is delivered by the short-wave radiation balance is primarily controlled by the albedo, which covers a range of values between 0.9 for fresh fallen snow and 0.3 for firn or even 0.15 for bare ice. At a high mountain site, the contribution of the radiation balance during a clear day in the summer may rise up from 80 to 90 percent of the energy available for melt, which amounts to more than 600 Wm<sup>-2</sup> (WEBER 2005). Almost the complete carryover of the right side of the energy balance equation is distributed to the turbulent fluxes of sensible and latent heat.

Due to the fact that fresh fallen snow reflects up to 90% of the incoming short wave radiation, the fraction of the absorbed energy is comparable to the magnitude of the turbulent fluxes, i.e. within a range of approx. 50 - 150 Wm<sup>-2</sup>. For this reason a correct determination of both the sensible and the latent heatflux should be achieved. This is especially important since under conditions of large radiation input and simultaneous presence of cold and dry air ablation is mainly caused by sublimation. However, the question remains how the turbulent fluxes can take on the high values despite of the very stable stratification of the near surface layer.

Over inclined terrain the development of a typical catatic flow can be frequently observed. It is characterized by a low level jet near the surface which is incompatible with the assumption of a constant flux layer, but the latter represents one of the most stringent assumptions for the application of the similarity theory (MONIN & Obukhov 1958; STULL 1988).

Furthermore, one can learn by observation that the catatic flow shows an intensive turbulent motion, as long as the mean wind speed does not exceed critical values which depends on the local conditions (WEBER 2005). With increasing speed the character of the flow

becomes more and more laminar, and the efficiency of the turbulent transport is reduced. A sophisticated parameterization scheme should consider this process.

This paper shows a practical approach, based on results of experimental investigations HyMEX98 and HyMEX 2000, which were carried out on an alpine glacier in 1998 and 2000 (WEBER 2005, BRAUN et al. 2004, ESCHER-VETTER & WEBER 2000).

## 2. Common methods to determine the turbulent fluxes

In contrast to the radiative fluxes the turbulent fluxes cannot really be directly determined by a physical method. However formulas are well established which result from the hydrodynamic model known as the set of the primitive equations. Thus the sensible heat flux **H** and the latent heat flux **LE** can be calculated by

$$H = -\bar{\rho} \cdot c_p \overline{w'T'} \quad [2.1] \quad \text{and} \quad LE = -\bar{\rho} \cdot l_v \overline{w'q'} \quad [2.2]$$

with mean density **ρ**, heat capacity of air **c<sub>p</sub>**, vertical wind speed **w**, air temperature **T**, latent heat of vaporisation **l<sub>v</sub>** and specific humidity **q**. The overbar symbol indicates an instruction for averaging the argument over an adequate time period, which depends simultaneously on the scale of the largest element of the turbulent motion and the mean speed of the flow. It intuitively follows from an idea of G.I. TAYLOR (1938), the so-called *Taylor's Hypothesis of Frozen Turbulence* which is a transformation of the attributes of the elements of the turbulent motion to a time series of a measured quantity, and vice versa. In this sense *frozen* is a synonym for *stationary*. This concept of a model of near surface turbulence establishes the general basis for the *Eddy Correlation Method* (ECM) which will be later discussed.

The primes denote the actual deviation of a quantity from the average over the period mentioned above. The mean value is equivalent to the well known variance. Multiplication and averaging the timeseries of the deviation of two quantities, e.g. the vertical wind speed component **w** and the air temperature **T** finally leads to the covariance, which is defined as the so-called *kinematic flux* of sensible heat. Finally, the multiplication by the mean density **ρ** and the heat capacity of air **c<sub>p</sub>** delivers the heat flux in Wm<sup>-2</sup>. The moisture flux can be accordingly determined, using the quantities **w** and the specific humidity **q** to get the kinematic flux, and the latent heat of vaporisation **l<sub>v</sub>** instead of **c<sub>p</sub>** to calculate the latent heat flux **LE**.

Equations 2.1 and 2.2 are valid at any location, time and level above the surface, but in practice, they are not easily applicable. It requires enormous data recordings of very high accuracy and resolution in time. Hence, the following approach is commonly used, based on the analogy to molecular heat conduction:

$$H = \bar{\rho} \cdot c_p \cdot K_H \frac{\partial \bar{T}}{\partial z} \quad [2.3] \quad \text{and} \quad LE = \bar{\rho} \cdot l_v \cdot K_{LE} \frac{\partial \bar{q}}{\partial z} \quad [2.4]$$

As the kinematic flux is replaced by the vertical gradient of the mean temperature  $\mathbf{T}$  or the specific humidity  $\mathbf{q}$  multiplied by a turbulent exchange coefficient  $\mathbf{K}$ , the approach is well known as *profile method* or *K-approach*. The overbar symbol indicates the identical procedure for aggregation as defined in eq. [2.1/2]. The potentially differing coefficients  $\mathbf{K}_H$  (sensible heat) and  $\mathbf{K}_{LE}$  (latent heat) can be determined by comparison of eq. [2.3/4] with eq. [2.1/2], but the validity of the result would be local.

If the fluxes are constant with height, the profile can be integrated and the turbulent efficiency of the exchange coefficient may be calculated depending on properties of the profile of wind speed and the thermal stability of the surface layer (STULL 1988). Using the *similarity* theory (MONIN & Obukhov 1958) the interrelation is described by *universal stability functions*, which were determined empirically (e.g. BUSINGER et al. 1971, DYER 1974). The validity of this function is now well proven for neutral and unstable layering but it fails under the conditions of a stable surface layer and especially within catabatic flows. What remains is only the fact that the calculation of the turbulent fluxes depends on a variable, which characterizes the state of the flow, and on the vertical profiles of temperature, humidity and wind speed. Among others, e.g. OERLEMANS (2001) introduced further simplifications of eq. [2.3/4]:

$$H = \rho \cdot c_p \cdot C_H \cdot U \cdot (T - T_0) \quad [2.5]$$

and respectively

$$LE = \rho \cdot l_v \cdot C_{LE} \cdot U \cdot (q - q_0) \quad [2.6]$$

whereas  $\mathbf{U}$ ,  $\mathbf{T}$  and  $\mathbf{q}$  now represent the time-aggregated horizontal wind speed, air temperature and specific humidity at a well defined level (in general at 2 m above the surface). Variables provided with a zero-Index denote the values directly on the snow surface. Equations of this type are frequently called *bulk formulae*.  $C_H$  and  $C_{LE}$  are not equal to  $\mathbf{K}_H$  and  $\mathbf{K}_{LE}$  in eq. [2.3/4], but are simple functions or constants derived from experimental results and adapted to the location where they are applied.

In spite of the strong simplifications, the bulk formulas of eq. [2.1/2] and [2.3/4] still consider the essential interrelations of turbulent transport: the dependency from air density, wind speed and stability.

Parameterizations of this type are widely and successfully used in melt water production models. At larger scales, even simpler models are used to calculate the sensible heat flux (e.g. ESCHER-VETTER 2000, STRASSER et al. 2002, STRASSER et al. 2006 (this volume)):

$$H = 5.7 \cdot \sqrt{U} \cdot (T - T_0) \quad [2.7]$$

Eq. [2.7] is normally used to approximate the sensible heat flux in catchments situated in mountainous regions. Compared to eq. [2.5] it has evident failings. The first three variables on the right side of eq. [2.5] were condensed to one single constant, which was derived using data measured at an elevation of approx. 2800 m a.s.l. (Weissfluhjoch). Hence the formula shows no more explicit dependency of the flux on altitude, but only indi-

rect through the temperature decrease with height. The formula may be applicable in small areas with a limited elevation range. For areas with an elevation range of more than 2000 m, methodical errors in the determination of the sensible heat flux of up to 30% have to be accepted due to the decrease of air density.

Using eq. [2.7] an increasing wind speed results in larger sensible heat fluxes following the idea that higher wind speed leads to a higher intensity of the turbulence. However, above a critical threshold the flow becomes more and more laminar and therefore the turbulent transport becomes less efficient. This effect is taken into account by reduction of the influence of the wind speed with the square root function.

The knowledge of accurate values of surface temperature and humidity during melting conditions can be seen as an important advantage, in contrast to only knowing the values 2 m above the ground which are tuned by the local processes of energy exchange. Temperature above a melting snow field is strongly reduced compared to the one above bare ground at the same elevation. Therefore one has to take care in the modelling if a field of temperature and humidity is interpolated using gradients between a few stations. This procedure may cause methodical errors, if there are significant subscale deviations of the resulting temperature field. But as further discussed in the following paragraphs, the calculated fluxes are not valid at a local point, but represent a mean value averaged over an upstream area (fetch) of a minimum of  $10^4 \text{ m}^2$  up to more than  $1 \text{ km}^2$ . Therefore it may be better for the accuracy of model results to use as input for the equations similar "representative mean values" instead of local measurements.

### 3. Eddy Correlation measurements and time series analysis

To prove the validity of the methods described in paragraph 2, a reference value of the kinematic flux is needed. An approach to determine it directly is given by the well known *Eddy Correlation Method*. It is based on the idea to translate the information about the spacial structure of turbulence to a function of time using the mean wind speed. The theoretical background was given early by TAYLORS hypothesis. The postulate of stationarity of the flow means: an isolated element of turbulent motion (eddy) has to evolve and to persist while passing the sensor. A simplified illustration of the principle is shown in Fig. 1. A more detailed description of the basics can be found in STULL (1988), Foken (2003) or WEBER (2005). Thus, the method delivers information only along a cross-section, which is in line with the upstream medium wind direction. The extension of the result from the line to an area requires the additional assumption of lateral homogeneity.

The determination of the fluxes of sensible and latent heat requires technically highly developed sensors. A 3-dimensional ultrasonic anemometer is required to measure the fluctuations of each component of the wind vector with sufficient precision and frequency. The sa-

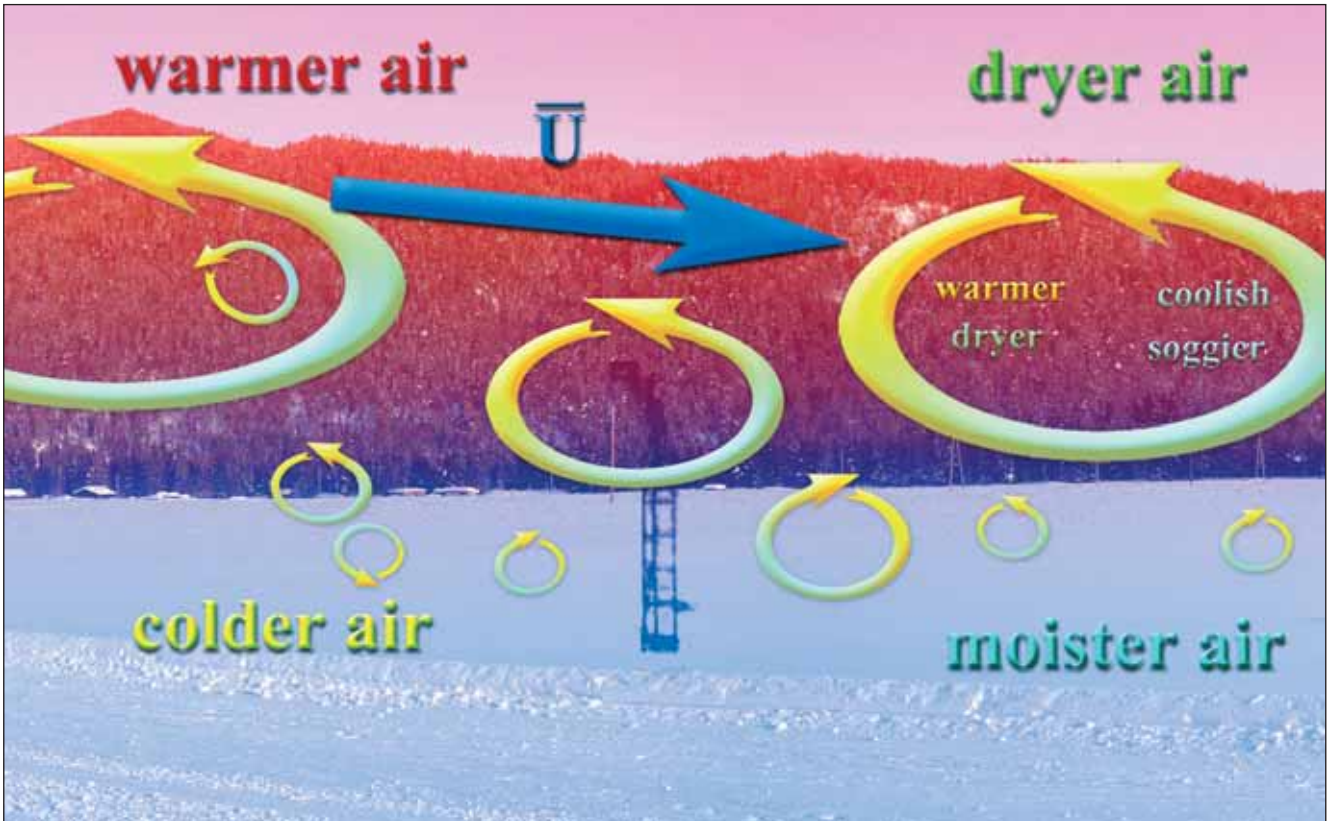


**Figure 1:** The principle of the eddy correlation method: elements of turbulent motion (so-called eddies), which are embedded in a turbulent flow with a mean wind speed  $\bar{U}$ , are passing a fixed sensor. An isolated element has to evolve and to persist while passing the instrument. The attributes of the air within the domain of influence of the eddy were translated to measured time series of the quantities

me instrument is able to measure the fluctuations of the (virtual) temperature which has to be corrected due to the influence of the fluctuations of water vapour to get the (potential) air temperature. Measurement of the fluctuation of the specific or absolute humidity requires a separate sensor, e.g. an instrument working on the principle of absorption of monochrome light by water vapour. Especially the spectral line of Krypton or Lyman- can be used successfully.

Required frequency for the measurements of a discrete time series of the wind vector components, the air temperature and humidity is in the range of 30 to 100 samples per second (Hz). As a first approximation the kinematic flux can be calculated using

[3.1] for sensible heat

$$\overline{w'T'} = \frac{1}{N-1} \left[ \sum_{k=1}^{N-1} w_k \cdot T_k - \frac{1}{N} \left( \sum_{k=0}^{N-1} w_k \sum_{k=0}^{N-1} T_k \right) \right]$$

[3.2] and for latent heat

$$\overline{w'q'} = \frac{1}{N-1} \left[ \sum_{k=0}^{N-1} w_k \cdot q_k - \frac{1}{N} \left( \sum_{k=0}^{N-1} w_k \sum_{k=0}^{N-1} q_k \right) \right]$$

The variable  $N$  denotes the count of numbers of the time series, which covers the required period for averaging. E.g., using a sampling rate of 20 Hz, it may range from

36.000 to 72.000. From the horizontal components of the wind speed the friction velocity  $u_*$  can be calculated by substitution of the scalars in eq. [3.1] by the horizontal cartesian wind vector components  $u$  (W – E) and  $v$  (N – S) and

$$u_*^2 = \sqrt{u'w'^2 + v'w'^2} \quad [3.3].$$

$u_*$  is an informative parameter to consider the influence of the aerodynamical roughness of the surface and the fraction of the mechanically induced turbulence.

From the theoretical point of view the eddy correlation method seems to be speciously simple. The sums in eq. [3.1 – 3.3] can be easily calculated in real time during data acquisition and after  $N$  measurements are captured, values for the turbulent fluxes are immediately available. But that is only half the truth. First of all the algorithm listed above is based on strong simplifications and the experimental data has to fit to the special requirements of the spectral model of turbulence. This will be discussed in the next section. Secondly the instruments have a lot of malfunction sources. Therefore in practice it is an exhausting procedure to get usable data sets and results. This is especially the case for the measurements over melting surfaces under cold and wet weather conditions.

Because of the difficulty to align the sensor in a fixed position there is an imperative need for an additional pro-

be, which records the inclination of the instrument setup continuously. Frost-covered sensors are the main reason for frequent break downs of the instruments and gaps in data series. An unfavourable signal-to-noise ratio leads to a reduction of the quality and of the high temporal resolution of the measurement signal. Additional difficulties are wind shadowing effects by the probe itself and errors due to an inevitable displacement of different instruments. To minimize these errors e.g. a special rotor system was developed which automatically adjusts the probe to the best position with respect to the direction of the incoming air flow. A suitable equipment to measure covariances is shown in Fig. 2. It was used during the HyMEX98 experiment on Vernagtferner. More details concerning the experimental experiences, description of technical problems and possible solutions can be found in WEBER (2005).

Eddy correlation measurements were carried out not only to determine the fluxes, but also to investigate the physical nature of the turbulent exchange processes. The internal conditions within the atmospheric surface layer over a melting snow or ice surface differ distinctly from those over a bare ground surface. In the latter case layering is unstable, the location of the source for heat is well defined, but the location of the heat sink is situated above but it extends to the entire boundary layer. Besides the mechanically generated turbulence by friction

forces additional turbulent motion is well developed by buoyancy forcing. The eddy size increases with height. Under strong convective condition there is a disposition to form large coherent organized structures (e. g. "plumes", STULL 1988), which are embedded within the flow and make the heat transport very efficient.

In the case of a melting surface the situation is contrary: the location with sources for heat within the atmospheric boundary layer is not exactly locatable and may be in the upper part of the surface layer or in some cases above it. Even a complete decoupling of the surface layer from the upper layers can be observed. However, for the sink of heat the bottom is a clearly defined location. Thermal layering is extremely stable, and as a result, vertical movement is strongly constrained. Stimulation of turbulence by buoyancy forces is nearly impossible and is generated only mechanically by shear stress. The required kinetic energy of the turbulent motion has to be extracted from that of the mean flow, which will be reduced in speed. Hence catabatic down flow is an important source for turbulence within the stable surface layer.

Nevertheless, similarly organized structures can be detected within the stable layer over a melting surface as under convective conditions. They can be found as mainly three types of patterns in the high resolution time series of temperature or humidity as shown in Fig. 3: *ramp structures*, *waves* and *spikes*. The ramp structure is similar to that of a convective plume (KAIMAL & BUSINGER 1970), but its temperature record seems to be mirrored on the time axis (WEBER 2005). It illustrates the event of the special mixing process by entrainment of warmer air from layers above. Within a period of 30 to 60 seconds the layer becomes colder because of the continuous extraction of heat at the snow or ice surface and mixing of air upwards by the turbulence. At the sharp edge the cold air mass will suddenly be replaced by new warm air from above, and the process is repeated. Therefore the main effect of the catabatic plumes is to destruct the stable stratification. The function of the *spikes* is similar; they transport cold air from the bottom upwards. Wave patterns can be particularly found within the transition period around sunrise and sunset: The stable stratified air mass is initiated to oscillate. But as there is no correlation to vertical movements, no forcing enhancement of the turbulent transport can be expected.

#### 4. Spectral analysis and flux calculations

Present understanding of the turbulent transport is strongly affected by the applied modelling concepts. To avoid misinterpretation, the conformity of the results with the model used should be proven. The model of atmospheric turbulence used for that purpose here is based on VAN DER HOVEN'S energy (variance) spectrum (VAN DER HOVEN 1957). As shown in Fig. 4, this spectrum of periodical motion can be divided in 4 well defined ranges with selected types of turbulence which



**Figure 2:** System for eddy correlation measurements, which is mounted on a 2 m tower and run continuously during 5 day periods in August 1998 and 2000, respectively, at Vernagtferner (Oetztal Alps, Austria) at an elevation of 3000 m a.s.l. The glaciologist in Markus Weber, the author. (Photo by Jan Greune)

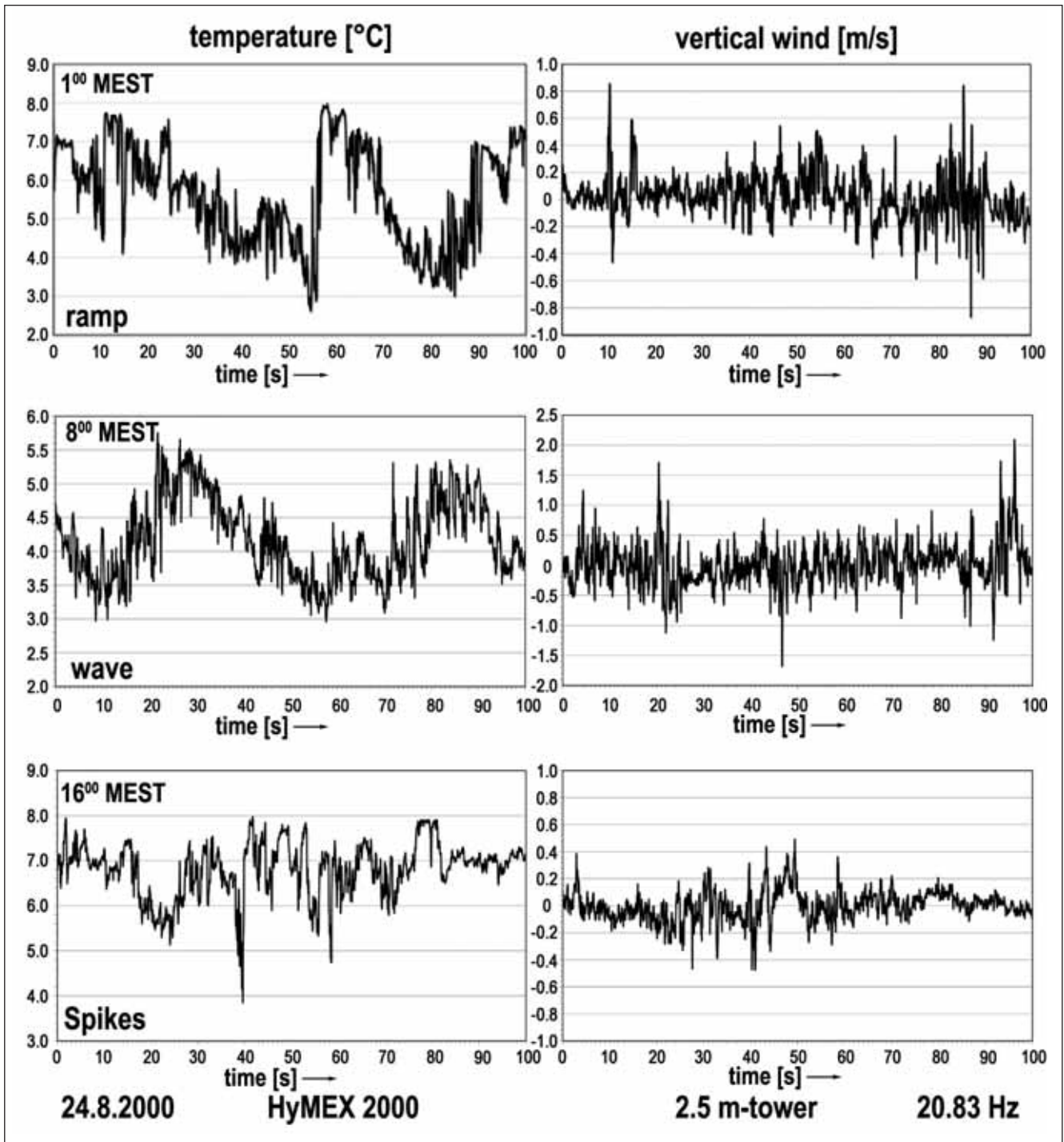


**Figure 3:** Examples of simultaneous 20.83Hz time series of air temperature and vertical wind speed, measured over a melting surface (Vernagtferner, Austria). Positive values for the vertical wind are directed upwards. The temperature data show examples of characteristic pattern within a stable layer (adapted from WEBER 2005)

each has typical properties with respect to life time and dimension.

The vertical transport occurs within the range of the micro-scale turbulence. It can be divided into a section where energy is generated and another where energy is dissipated, according to the denotations “buoyancy forced” and “mechanically generated” used in paragraph 3. The resulting value of the covariance respectively, which is determined using the statistical procedure de-

scribed above, needs an additionally analysis of the data to be interpreted properly as a turbulent heat flux. Therefore the result of the spectral analysis used here has to show satisfactory agreement to this model of the micro scale turbulence.

In addition it is a useful tool

- to test the raw data series for signal errors and noise; a closer look on the decline within the inertial subrange of the variance spectra reveals whether the sampling

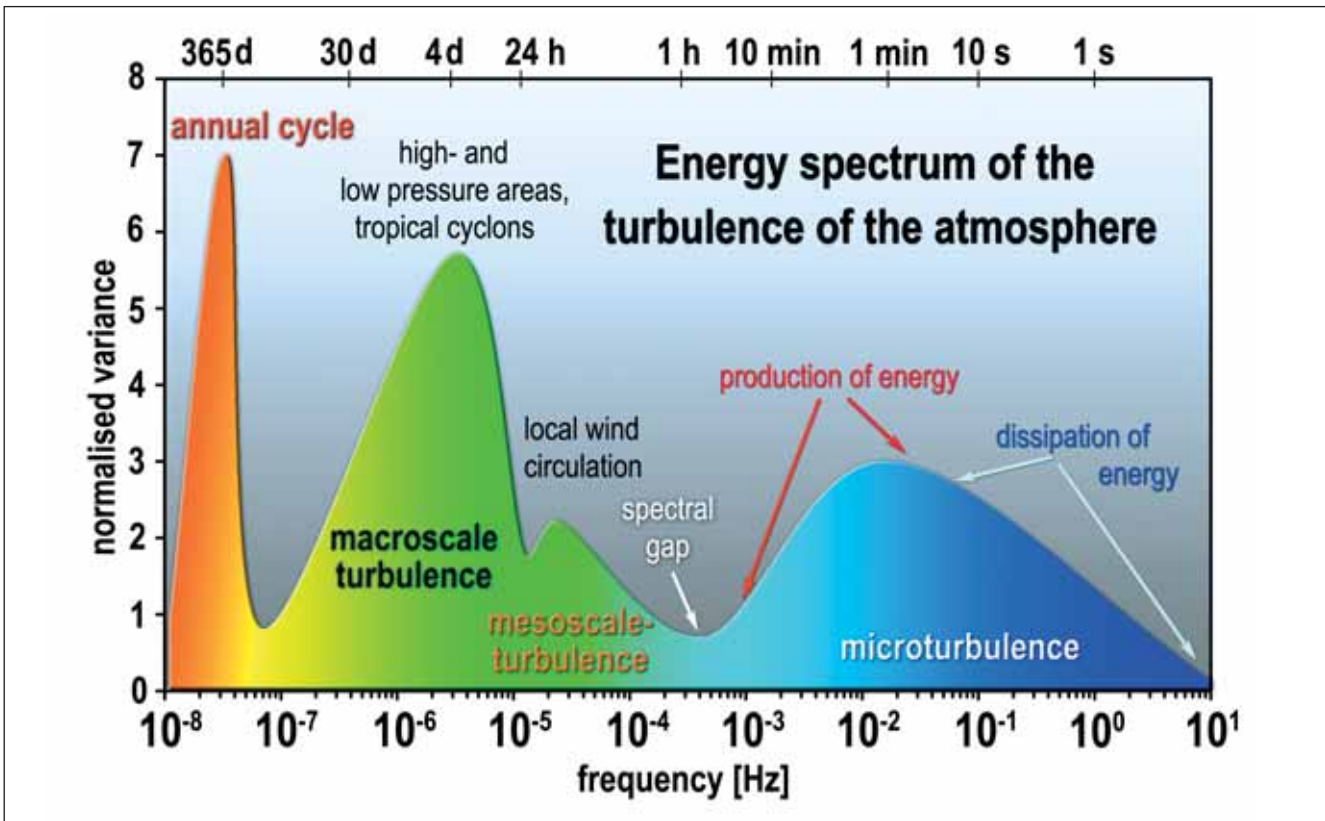


**Figure 4:** Schematic illustration of a 3-year atmospheric turbulence variance spectrum of the horizontal wind speed. The processes of turbulent heat exchange cover the blue colored frequency range of the microturbulence, separated from large scale circulations by a distinctive minimum (spectral gap). The figure is based on VAN DER HOVEN (1957) and ROEDEL (2000)

frequency and the data accuracy of the sensors are sufficient;

- to determine essential corrections to the obtained variance and covariance;
- to analyse the structure of the turbulent flow and the transport processes by comparing the spectra among each other and to the well known standard spectra.

The coefficients  $S(n)$  of the variance spectra (sometimes denoted also as power spectrum) from a discrete time series  $f(k)$  with  $N$  numbers of equidistant and successive values (now gaps are admitted) can be determined by the common Fourier Transformation

$$S(n) = \sum_{k=0}^{N-1} \frac{f(k)}{N} \exp(-i2\pi nk/n) \quad [4.1]$$

Summation over all the coefficients of the power spectrum results in the total variance  $\sigma^2$  of the time series

$$\sigma^2 = \sum_{n=1}^{N-1} S(n) \quad [4.2]$$

To computationally transform the time series to the variance spectra the common FFT-algorithm (*Fast-Fourier-Transformation*) is used, which is highly efficient, but normally this restricts the length of the data sets of  $N=2^m$  values, where  $m$  is an integer.

To analyse and compare the spectra they can be graphically presented in an appropriate way. Standardisation

and normalisation can be performed by multiplication of the spectral coefficients with the frequency  $f$  and subsequent scaling with the total variance. Plotting of such spectral curves using a semi-log axis has the advantage that the fraction of the area below the curve is proportional to its contribution to variance. An example is shown in Fig. 5, where the variance spectra of the fluctuation of temperature, humidity, vertical and horizontal wind speed are compared. Clear differences within the high frequency range of the scalar quantities and the horizontal wind speed are errors in the signal. The horizontal course of the humidity spectrum at the end of the inertial subrange indicates random noise at frequencies above 0.3 Hz.

Using a log-log axis for plotting, all normalised spectra should merge together. KAIMAL AND FINNIGAN (1972) and KAIMAL et al. (1994) have prepared standardised spectra adapted to the condition of a stable surface layer on homogeneous terrain. The example in Fig. 6 shows very good agreement of the spectra, measured at different location and time at Vernagtferner (Austria). At frequencies higher than 10-2 Hz the spectra also fit very well with the standard spectra. That means the basic turbulence theory might be fulfilled. But the range of energy production shows characteristic deviations which can be related to the special entrainment processes mentioned above. In addition, the maximum size of the eddy seems to be limited to the dimension of the melting surface.

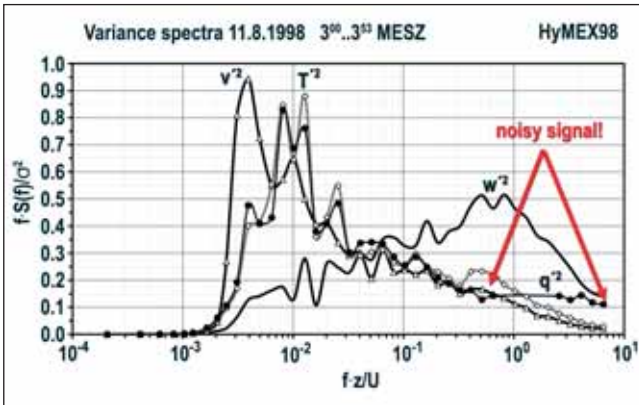


**Figure 5:** Normalised variance spectra of air temperature (T), specific humidity (q), horizontal wind speed (v) and vertical wind speed (w). The labelled section within the inertial subrange of the spectra of q clearly indicates some noise, which is superimposing the signal

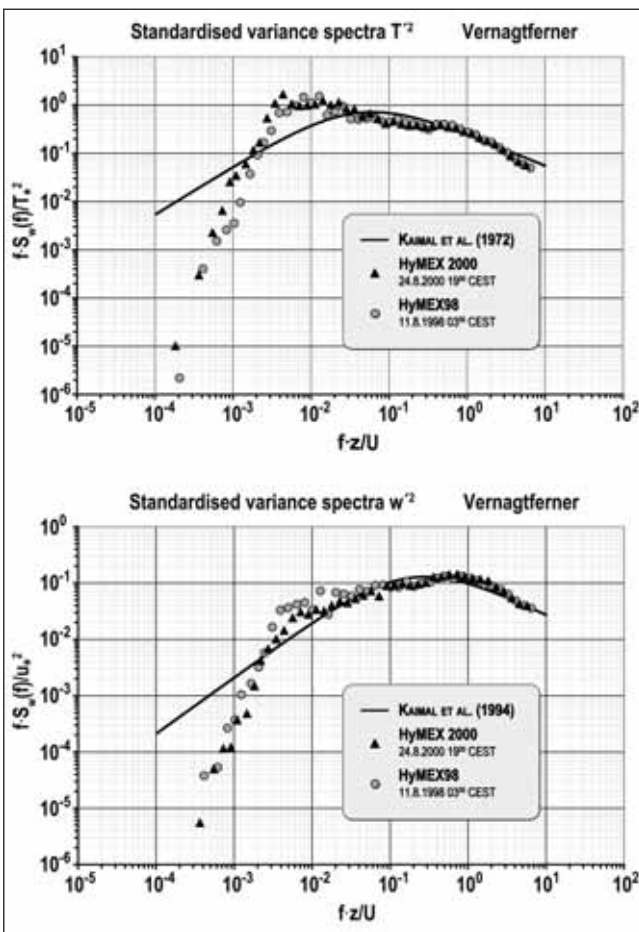


**Figure 6:** Standardised variance spectra of air temperature (top) and vertical wind speed (bottom) in comparison with standard spectra according to KAIMAL et al. (1972) and KAIMAL AND FINNEGAN (1994)

The kinematic flux is defined by the covariance and therefore by the integral of the cospectrum. It can be discretely calculated using the real part (Re) and the imaginary part (Im) of the concerned quantities:

$$[4.3].$$

$$Co_{ab} = \text{Re}(S_a) \cdot \text{Re}(S_b) + \text{Im}(S_a) \cdot \text{Im}(S_b)$$

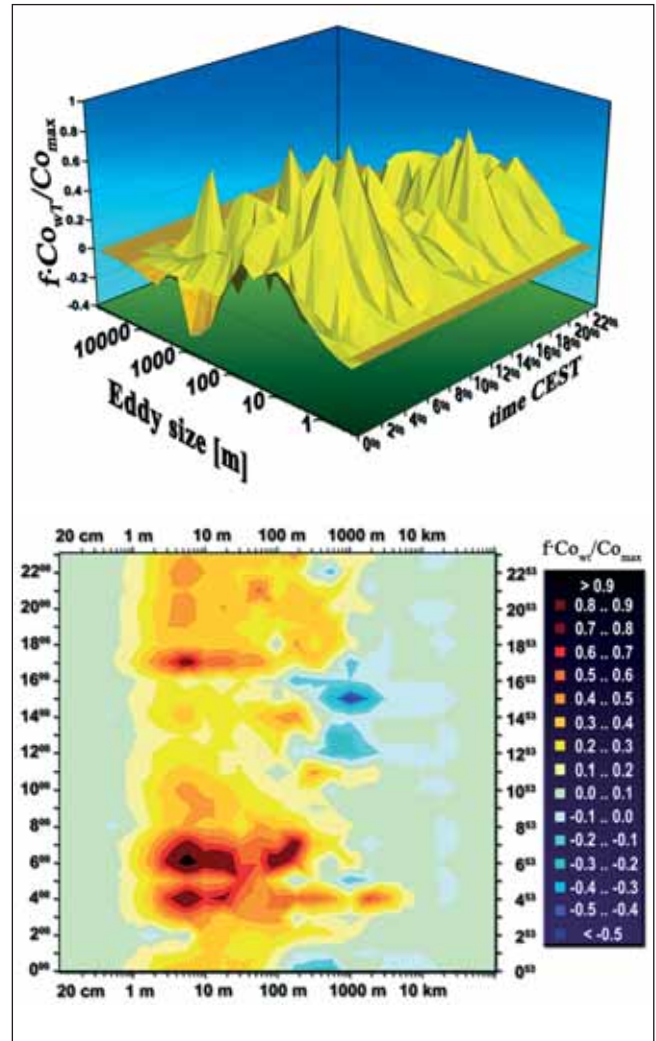


**Figure 7:** Diurnal variation of normalised cospectra of the sensible heat flux (Vernagtferner, Austria)

Standardisation of the cospectra using the mean wind speed as a scaling factor enables the illustration of the footprint and the detection of the source area of the flux. Fig. 7 shows the distribution of the flux intensity of the sensible heat versus the characteristic eddy size and time. Mapping the result clearly shows that the fetch for the main fraction of the flux is within a distance of 500 m upwind. The maximum of the sensible heat flux occurs in the period at the second part of the night when the catabatic forcing becomes maximal. At noon one can detect bands where the contribution of the flux becomes negative. These have their source at limited snow free areas in the summit regions, where a hot rock surface enables ascending air masses forced by convection. This contribution has to be removed from the total covariance as it is not related to the melting surface. The amazing analogy between the turbulent structure of the enthalpy distribution and that of moisture suggests that the area below the standardised cospectrum of the sensible heat has to be congruent with that of the latent heat. If not, this may be an indicator of technical errors or an inadequate response time of the probe. As shown in Fig. 8, the close correlation between the fluctuation of air temperature and humidity justifies the application of

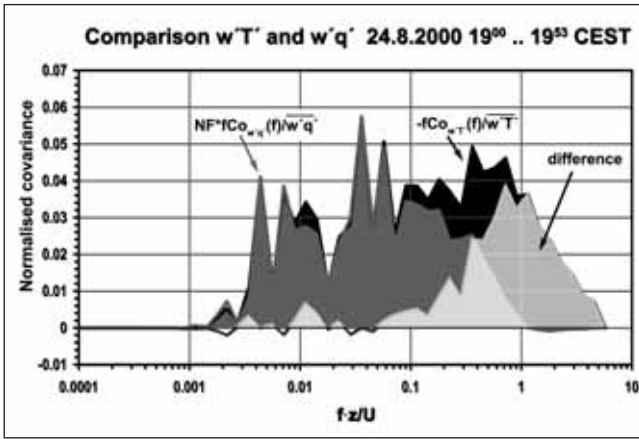


Figure 8: Comparison between the normalised cospectra of sensible and latent heat (Vernagtferner, Austria)

the following procedure based on the *Bowen ratio* (Bowen 1926) to estimate the covariances of the latent heat flux proportional to that of the sensible heat flux:

$$\overline{w'q'} = \overline{w'T'} \frac{\sigma_q}{\sigma_T} \quad [4.4]$$

Since there are much more difficulties to measure humidity fluctuations than these of temperature or wind speed, eq. 4.4 seems to be a suitable approach to fill inevitable gaps in the data recordings.

## 5. A bulk-parameterization approach of the turbulent fluxes

Extensive analysis of experimental data leads to the conclusion, that the concept to model the turbulent transport presented here may be suitable (WEBER 2005). In the following, the parameterizations are tested and improved.

First it is a fact that the covariance can be split into the product of a correlation coefficient  $R$  and the variances of each component:

$$\overline{a'b'} = \sum_{k=0}^{N-1} Co_{ab}(f_k) = R_{ab} \cdot \sigma_a \cdot \sigma_b \quad [5.1]$$

This approach is better known as the “flux-variance-relationship” (FOKEN 2003). It is assumed that a satisfying relationship of the following type can be found:

$$\sigma_T \approx T - T_S \quad \text{and} \quad \sigma_w \approx \sigma_u \approx \overline{U} \quad [5.2]$$

Then the following simple bulk-equation can be derived:

$$H = \rho \cdot c_p \cdot R_{wT} \cdot f(U) \cdot f(T - T_0) \quad [5.3]$$

Eq. 5.3 has a similar structure to the one of eq. 2.5. The main difference is the unknown correlation coefficient  $R$  which must have a close relation to the exchange coefficient  $C$  of eq. [2.5].

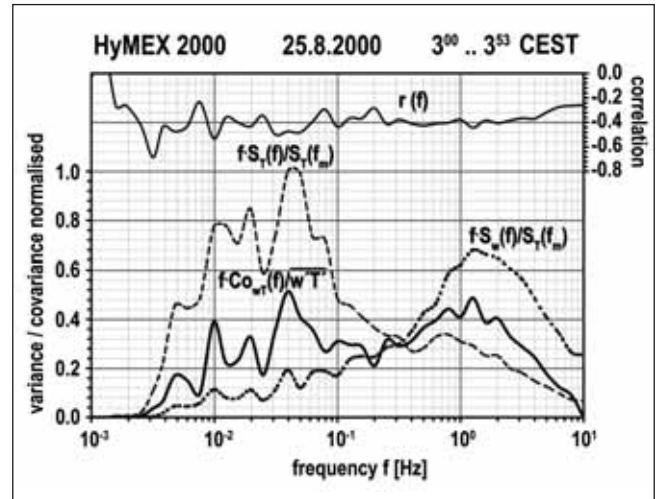


Figure 9: Combination of the cospectra  $w'T'$  derived from the variance spectra of  $T$  and  $w$ . On top: the resulting coefficient of correlation (Vernagtferner, Austria)

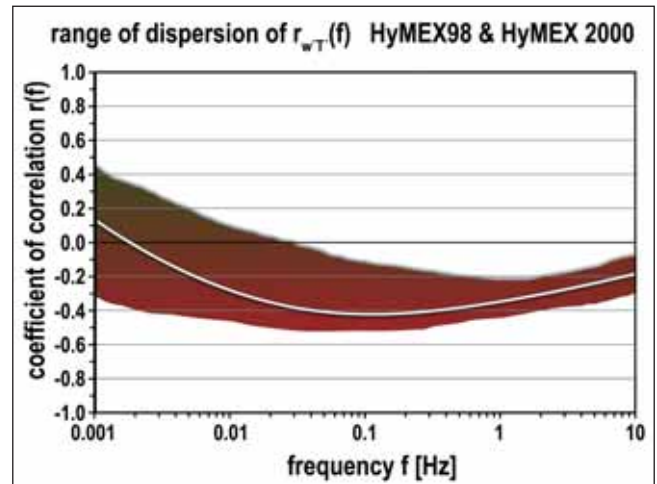


Figure 10: Range of dispersion of the correlation coefficient between the variances of temperature and vertical wind speed based on 240 samples (Vernagtferner, Austria)

Fig. 9 shows that  $R$  is not a significant function of frequency. It can be seen that it is almost constant over the entire frequency range. But there may exist an important dependency on the intensity of turbulence and therefore on atmospheric stability. The observed range of dispersion of the correlation coefficient based on the entire dataset of the experiments HyMEX98 and HyMEX2000 (240 values) is depicted in Fig. 10. The maximal variation can be found at the range of frequencies which equals that for production of energy. Thus a simple linear function must be sufficient to approximate the influence of the stability to the mean correlation coefficient.

The necessary functions can be determined by a simple linear regression analysis (Fig. 11). Equations [5.5] to [5.6] are simple bulk functions to calculate sensible and latent heat flux, the constants are empirical. The correlation coefficient can be replaced either by a constant value estimated  $R_{wt} = -0.35$ , or better by the result of eq. [5.4] which considers the observed influence of the relationship between stability, wind speed and turbulence evolution.

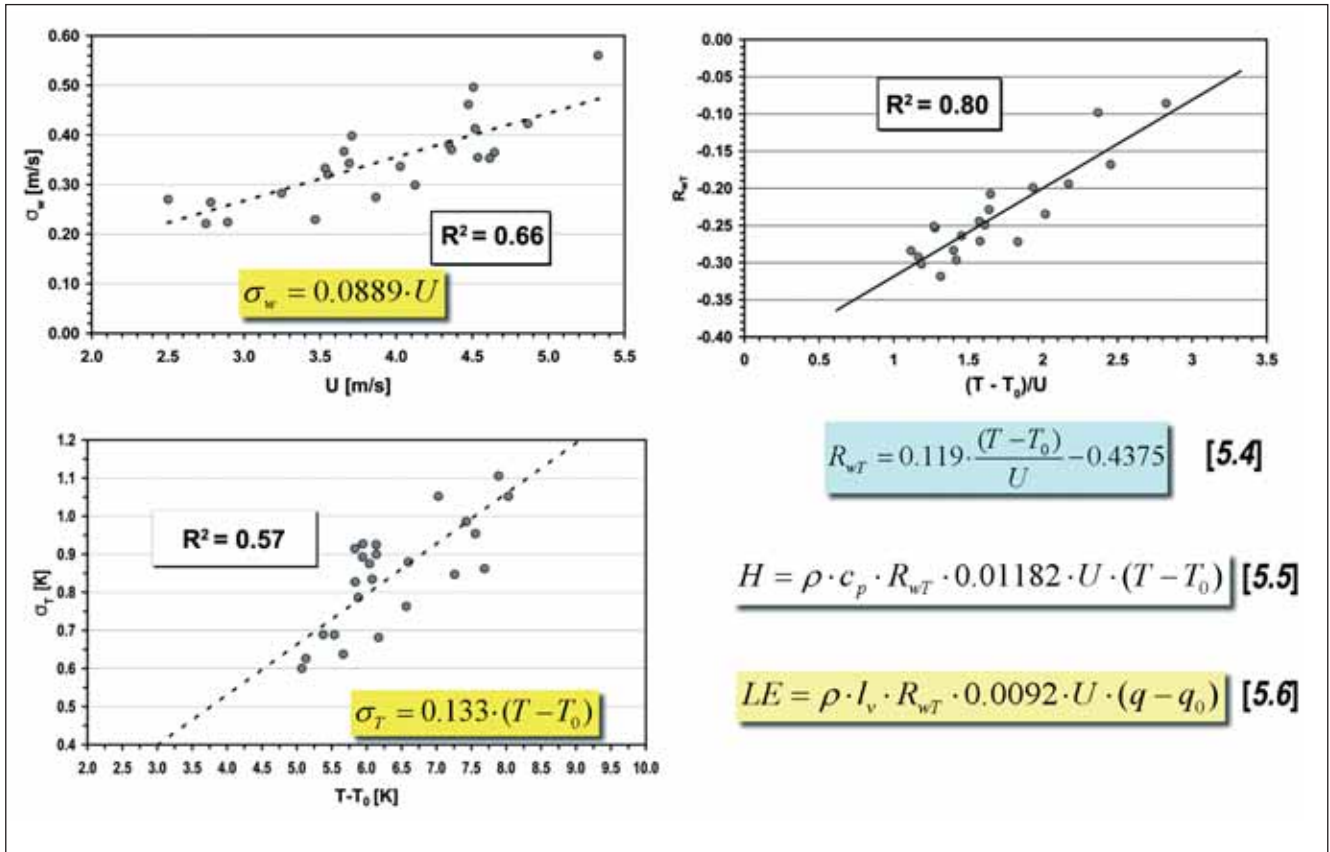


Figure 11: Regression analysis to derive bulk formulas for the sensible and latent heat fluxes (data from Vernagtferner, Austria).

Table 1: Daily mean values of the sensible heat flux  $H$  [ $W/m^2$ ] at two different locations 2.5 m a.g. at Vernagtferner determined by different methods. 1): reference flux directly calculated from eddy correlation measurements ( $\pm$  estimated range of error); 2) flux calculated using eq. [2.7] and hourly means of air temperature, surface temperature and wind speed at 2.5 m a.g.; 3) application of the parameterization eq. [5.5] and a constant value  $-0.35$  for the correlation coefficient.  $R$ ; 4) utilization of eq. [5.5] and additionally of the parameterization of the correlation coefficient  $R$  using eq. [5.4]. (Excerpt from WEBER 2005)

Date	9.8.1998	10.8.1998	11.8.1998	24.8.2000	25.8.2000	26.8.2000
ECM flux <sup>1)</sup>	27.5 $\pm$ 15	34.7 $\pm$ 15	41.0 $\pm$ 15	61.7 $\pm$ 10	60.0 $\pm$ 10	45.8 $\pm$ 15
Eq. [2.7] <sup>2)</sup>	77.93	82.95	82.41	71.40	62.50	63.50
$R_{wt}=0.35$ <sup>3)</sup>	49.96	83.02	54.80	79.69	71.26	54.80
Eq. [5.5] + [5.4] <sup>4)</sup>	29.64	36.89	48.63	67.40	68.07	55.37

Table 1 gives criteria of assessment to the performance of the different parameterizations by comparing daily means of the fluxes to the directly measured reference. The methods neglecting the influence of the turbulence efficiency, the simple approach eq. [2.7] and eq. [5.5] using a constant correlation coefficient tend toward overestimate the real sensible heat flux. Introduction of the square root of the horizontal wind speed is not sufficient to correct the effect of the flow to get more and more laminar with increasing speed.

Additional sources of error result from not considering the local influence of the air density using eq. [2.7]. It can be seen by comparing the values of 1998 to that of 2000, which are archived at different locations and elevations. The more sophisticated parameterization [5.5] and [5.4] matches up best to the measurements.

An example of the application of the three different approaches to calculate the hourly diurnal variation of the fluxes of sensible and of latent heat is shown at Fig. 12. Comparison with the result from direct measurements shows the best fit by using the sophisticated parameterization. This is valid as well for flux of sensible heat as for the flux of latent heat, despite of some overestimation of the magnitude of flux near its maximum. Especially periods characterized by weak turbulence are not very well represented using algorithms, where the variation of the correlation coefficient is not considered. But overall all approaches used here are applicable for modelling the turbulent fluxes while accurate input data at 2 – 2.5m a.g. is available. To validate the approaches presented here, very accurate direct measurements has been used. This must be considered if the performance of the parameterization is estimated.

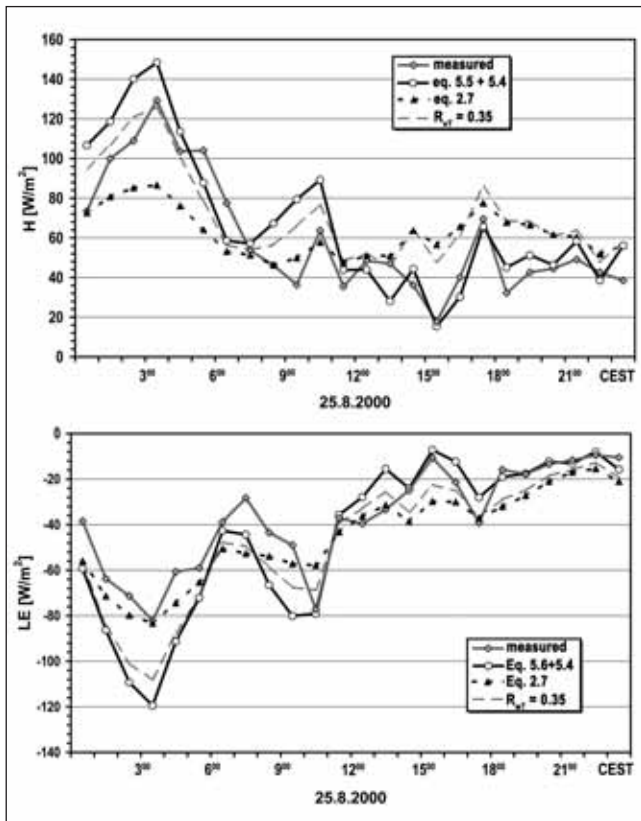


**Figure 12:** Application of the bulk approaches to calculate the sensible (top) and latent heat fluxes (bottom) using eq. 5.5, 5.4, 5.6, 5.4, 2.7, 5.5 and 5.6 with a constant  $R_s$ . Comparison with values measured by eddy correlation (Vernagtferner, Austria)

## 6. Conclusions

For distributed, physically based modelling of snow- or icemelt robust and accurate algorithms to calculate the energy balance terms are required. The formula to determine the turbulent fluxes presented here is now implemented into the snow model component of the Danubia decision support system developed in the GLOWA-Danube project (MAUSER & STRASSER 2005) where it seems to work successfully. It fulfils requirements like representing the dependence of the fluxes on altitude. Further it gives a better fit with the measurements than common approaches used so far.

The approach claims not be “universal”. Probably it is only applicable to the area where it was derived. Additional measurements may be expensive but could confirm the results found in this study.

## Acknowledgments

The author would like to thank all colleagues who contributed to this study and assisted during the field experiments. Financial support was provided by the German Research Foundation and Federal Ministry of Education and Research **bmb+f** as part of the GLOWA-Danube project.

## References

- BOWEN, I.S. (1926): The ratio of heat losses by conduction and by evaporation from any water surface. *Physical review*, 27, 779 – 787.
- BRAUN, L.N., ESCHER-VETTER, H., HEUCKE, E., SIEBERS, M & WEBER, M. (2004): Experiences with the new “Vernagtferner” hydro-meteorological station. In: OERLEMANS & TIJM-REIJMER: Book of extended abstracts of presentation at the Workshop “Automatic Weather Stations on Glaciers”, Pontresina, 28 to 31 March 2004, IMAU, 38 - 44.
- BUSINGER, J.A., WYNGAARD, J.C., IZUMI, Y. & BRADLEY, E.F. (1971): Flux-profile relationships in the atmospheric surface layer. *J. Atm. Sci* 28: 181 – 189.
- DYER, A.J. (1974): A Review of Flux-Profile-Relationships, *Boundary Layer Meteorology*, 7, 363-372.
- ESCHER-VETTER, H. (1980): Der Strahlungshaushalt des Vernagtferners als Basis der Energiehaushaltsberechnung zur Bestimmung der Schmelzwasserproduktion eines Alpengletschers. *Münchener Universitäts-Schriften, Fachbereich Physik - Univ. München Met. Inst. , Wiss. Mitt. Nr. 39*, 117 S.
- ESCHER-VETTER, H. (2000): Modelling meltwater production with a distributed energy balance method and runoff using a linear reservoir approach - results from Vernagtferner, Oetzal Alps, for the ablation seasons 1992 to 1995. *Zeitschr. f. Gletscherkunde und Glazialgeologie*, 36, 119-150.
- ESCHER-VETTER, H. & WEBER, M. (2000): Measuring and modelling the Vernagtferner energy balance components: results from HYMEX98 and the PEV model. *Snow and ice. Österreichische Beiträge zu Meteorologie und Geophysik 23* (2000) preprints, 111.
- FOKEN, T. (2003): *Angewandte Meteorologie – Mikrometeorologische Methoden*. Springer Verlag, Berlin, ISBN 3 540 00322 3, 289 S.
- KAIMAL, J.C. & BUSINGER, J.A. (1970): Case studies of a convective plume and a dust devil. *J. Appl. Meteorol.*, 9, 612-620.
- KAIMAL, J.C., WYNGAARD, J.C., IZUMI, Y & COTÉ, O.R. (1972): Spectral characteristics of surface-layer turbulence. *Quart. J. Royal Meteorol. Soc.*, 98, 563-589.
- KAIMAL, J.C. & FINNIGAN, J.J. (1994): *Atmospheric Boundary Layer Flows*. Oxford University Press, New York, 289S.
- KUZMIN, P.P. (1961): *Melting of snow cover*. Translated from Russian by Israel Program for scientific Translation, 1972, 290 S.
- MONIN, A.S. & OBUKHOV, A.M. (1958): Fundamentale Gesetzmäßigkeiten der turbulenten Vermischung in der bodennahen Schicht der Atmosphäre. In: GOERING, H. (Hrsg): *Sammelband zur statistischen Theorie der Turbulenz*. Akademie-Verlag, Berlin, 199-224.
- OERLEMANS, J. (2001): *Glaciers and Climate Change*. A.A. Balkema Publishers, Lisse/Abingdon/ Exton/ Tokyo, ISBN 90 265 1813 7, 148 S.
- OHATA, T. (1991): The effect of glacier wind on local climate, turbulent heat fluxes and ablation. *Zeitschr. f. Gletscherkunde und Glazialgeologie*, 25 (1), 49-68.

- STRASSER, U., ETCHEVERS, P. & LEJEUNE, Y. (2002): Intercomparison of two Snow Models with Different Complexity Using Data from an Alpine Site. In: *Nordic Hydrol.*, 33 (1), 15-26.
- ROEDEL, W. (2000): *Physik unserer Umwelt – die Atmosphäre*. Springer Verlag, Berlin, Heidelberg, 498S.
- STULL, R.B. (1988): *An Introduction to Boundary Layer Meteorology*. Kluwer Academic Publishers, Dordrecht, ISBN 90 277 2769 4, 666p.
- TAYLOR, G.I. (1938): The spectrum of turbulence. *Proc. Royal Soc. London*, A164, 476-490.
- VAN DER HOVEN, I. (1957): Power spectrum of horizontal wind-speed in the frequency range from 0.0007 to 900 cycles per hour. *J. of Meteorol.*, 14, 160 - 164.
- WEBER, M. (2005): *Mikrometeorologische Prozesse bei der Ablation eines Alpengletschers*. Dissertation, Institut für Meteorologie und Geophysik der Universität Innsbruck, 319p (<http://www.glaziologie.de/publikat/klima.html>)
- WEBER, M. AND KUHN, M. (2005): *Glowa-Danube: Modelling snow cover and glaciers within the catchment area of Passau-Achleiten gauge*. In: *GLOWA-Danube status report phase II, 2004 – 2005*, ([http://www.glowa-danube.de/PDF/reports/statusreport\\_phase2.pdf](http://www.glowa-danube.de/PDF/reports/statusreport_phase2.pdf))